AAS 12-639

HIGH-ORDER ANALYTIC CONTINUATION AND NUMERICAL STABILITY ANALYSIS FOR THE CLASSICAL TWO-BODY PROBLEM

Tarek Elgohary,* James D. Turner† and John L. Junkins‡

Several methods exist for integrating the Keplerian Motion of two gravitationally interacting bodies. Lagrange introduced three vector-valued invariants that allowed the position and velocity vectors to be expanded. Alternatively, the classical F & G Lagrangian coefficients provide a mapping of the initial position and velocity into current time values. Nevertheless, classically, it has proven difficult to develop high-order Taylor series expansions, even though the governing equations are well-defined. This work presents two scalar Lagrange-like invariants ($f = r \cdot r$ *and* $g = f^{-n/2}$) that enable all of the higher-order vector-valued derivatives to be recursively evaluated using Leibniz product rule. The calculations for the higher-order trajectory derivatives are developed by deriving a differential equation for g that eliminates fractional powers. The basic methodology is extended to handle perturbed acceleration force models for the J_2 zonal gravity harmonic term. The approach is both efficient and accurate. The two-body problem is handled by computing $\ddot{r} = -\mu r g$, where r = [x,y,z] denotes the inertial relative coordinate vector that locates an object relative to the Earth and μ = 398601.2 km^2/sec^2 is the gravitational constant. Given $r, \dot{r}, \ddot{r}$ Leibniz product rule is used to recursively develop $\{\dot{f}, \dot{g}, \ddot{r}\}, \{\ddot{f}, \ddot{g}, \dddot{r}\}, \cdots$. Series convergence issues are addressed by invoking a vector version of a Padé series approximation for each component of the vector-valued Taylor series $r(t+h) = r(t) + \dot{r}(t)h + \ddot{r}(t)h^2/2! + \dddot{r}(t)h^3/3! + \cdots$. The behavior of the Padé roots is studied as a function of the number of derivative terms retained in the series approximation and solution accuracy for the series approximation. Numerical results are presented that compare the solution accuracy and integration time required by *ODE45* and *RKN1210*, and the analytic power series methods developed in this work for two-body plus J_2 perturbation terms.

INTRODUCTION

Integrating the two-body equations of motion has been achieved applying several methods and algorithms. Lagrange invariants [1, 2] are one of the most famous approaches to utilize the recursive nature of the problem and combine it with Taylor series expansion. Several other approaches are

* Graduate Student, Aerospace Engineering, Texas A&M University, College Station, Texas 77843-3141.

† Research Professor, Aerospace Engineering, Texas A&M University, 745 HR Bright Building, 3141 TAMU College Station, Texas 77843-3141, U.S.A. E-mail: turner@aero.tamu.edu. Fellow AAS, Associate Fellow AIAA.

‡ Distinguished Professor, Texas A&M University, Aerospace Engineering Department, 722 H.R. Bright Build-ing, 3141 TAMU, College Station, Texas 77843-3141, U.S.A.
E-mail: junkins@tamu.edu. Tel. 979-845-3912; Fellow AAS.

readily available for the two-body problem solution. [3, 4, 5] Turner, et. al. have presented a Taylor series approach that computes an arbitrary order expansion using the scalar $f = \boldsymbol{r} \cdot \boldsymbol{r}$ and $g = f^{-n/2}$ Lagrange-like invariants. [6] Numerical results are obtained by using a combination of Leibniz rule and analytical Taylor series continuation to achieve mm accuracies in orbit calculations. The solution accuracy has been validated in both double and arbitrary precision simulations, where hundreds of digits of accuracy have been maintained in the solution for multiple orbits.

An interesting phenomenon is observed regarding the convergence behavior of the Taylor series that is related to a combination of the expansion order of the series, the step size and the precision of the calculations. Several numerical experiments showed that the series convergence reaches a point where it stops being affected by those factors. To examine this behavior, Padé approximations are utilized, [7, 8, 9] where the poles of the series are calculated and plotted for different cases. Understanding the poles behavior for different divergent and convergent cases is very important for investigating the overall series behavior.

The main contribution of the work is the development of an arbitrary order vector Taylor series approximation for the J_2 perturbed two-body problem of celestial mechanics. Numerical experiments with state-of-the-art integration algorithms indicate that the power series approach out performs the integration algorithms *200X*. The basic mathematical model for the perturbed two-body problem is presented first. Next, the recursive formulation for the Lagrange-like invariants is presented for both the two-body problem and the J_2 perturbation acceleration term. The results will be compared with existing high order numerical integrators in terms of accuracy and timing. Finally, the numerical stability of the series approximations is investigated by invoking a Padé series approximation, where the convergence and divergence issues for the series approximations are analyzed by comparing the pole behavior of the Padé series.

ANALYTIC CONTINUATION SOLUTION FOR THE PERTURBED TWO-BODY PROBLEM

The equation of motion for the perturbed relative two-body problem is given by,

$$\ddot{\mathbf{r}} = -\frac{\mu}{r^3}\mathbf{r} + \mathbf{a}_d \tag{1}$$

The disturbance acceleration term $\mathbf{a}_d$ referring to the J_2 effects arising from the Earth's oblateness is defined as,

$$\mathbf{a}_{J_2} = -\frac{3}{2}J_2\left(\frac{\mu}{r^2}\right)\left(\frac{r_{eq}}{r}\right)^2\begin{Bmatrix}\left(1-5\left(\frac{z}{r}\right)^2\right)\frac{x}{r}\\ \left(1-5\left(\frac{z}{r}\right)^2\right)\frac{y}{r}\\ \left(3-5\left(\frac{z}{r}\right)^2\right)\frac{z}{r}\end{Bmatrix} \tag{2}$$

where, $\mu = 398600.4418\ \text{km}^3 s^{-2}$ is the standard gravitational parameter of the Earth, $J_2 = 1082.63 \times 10^{-6}$ defines the oblateness perturbation, $r_{eq} = 6378.1370\ \text{km}$ is the Earth equatorial radius.

Two Lagrange-Like invariants are introduced to automate the process of generating arbitrary order time derivatives for the equation of motion in Eq. (1). The first Lagrange-Like invariant is defined as,

$$f = \mathbf{r}.\mathbf{r} \tag{3}$$

where (.) denotes the vector inner product. The n-th order time derivative of f is computed by applying Leibniz product rule as,

$$f^{(n)} = \sum_{m=0}^{n} \binom{n}{m} \boldsymbol{r}^{(m)}.\boldsymbol{r}^{(n-m)} \tag{4}$$

where $\binom{n}{m}$ is the standard binomial coefficient. The second Lagrange-Like invariant is given by,

$$g_p = f^{-p/2} \tag{5}$$

where the time derivative for Eq. (5) can be shown to be $f\ddot{g}_p + \frac{p}{2}\dot{f}\dot{g}_p = 0$. Evaluating the higher order time derivatives of g_p, using Leibniz product rule, one obtains,

$$g_p^{(n+1)} = -\left\{ \frac{p}{2} f^{(1)} g^{(n)} + \sum_{m=1}^{n} \binom{n}{m} \left(\frac{p}{2} f^{(m+1)} g^{(n-m)} + f^{(m)} g^{(n-m+1)} \right) \right\} / f \tag{6}$$

For the unperturbed problem, $\mathbf{a}_d = \mathbf{0}$, Leibniz rule is applied to evaluate higher order derivatives of $\mathbf{r}$ as a function of g_3 by computing,

$$\boldsymbol{r}^{(2+n)} = -\mu \sum_{m=0}^{n} \binom{n}{m} \boldsymbol{r}^{(m)} g_3^{(n-m)} \tag{7}$$

The J_2 perturbation acceleration is similarly represented as,

$$\mathbf{a}_{J_2} = \underbrace{-\frac{3}{2} J_2 \mu r_{eq}^2}_{\text{Constant (M)}} \begin{Bmatrix} x g_5 - 5xz^2 g_7 \\ y g_5 - 5yz^2 g_7 \\ 3z g_5 - 5z^3 g_7 \end{Bmatrix} = \text{M} \begin{Bmatrix} \ddot{x}_{J_2} \\ \ddot{y}_{J_2} \\ \ddot{z}_{J_2} \end{Bmatrix} \tag{8}$$

Several steps of Leibniz Rule are then applied to each element of $\mathbf{a}_d$ as follows,

$$
\begin{aligned}
x_{J_2}^{(n+2)} &= \sum_{m=0}^{n}\binom{n}{m}x^{(m)}g_5^{(n-m)} - 5\sum_{m=0}^{n}\binom{n}{m}\left(xz^2\right)^{(m)}g_7^{(n-m)} \\
&= \cdots - 5\sum_{m=0}^{n}\binom{n}{m}\left(\sum_{k=0}^{m}\binom{m}{k}x^{(k)}\left(z\cdot z\right)^{(m-k)}\right)g_7^{(n-m)} \\
&= \cdots - 5\sum_{m=0}^{n}\binom{n}{m}\left(\sum_{k=0}^{m}\binom{m}{k}x^{(k)}\left(\sum_{l=0}^{m-k}\binom{m-k}{l}z^{(l)}z^{(m-k-l)}\right)\right)g_7^{(n-m)}
\end{aligned} \tag{9}
$$

$$
y_{J_2}^{(n+2)} = \sum_{m=0}^{n}\binom{n}{m}y^{(m)}g_5^{(n-m)} - 5\sum_{m=0}^{n}\binom{n}{m}\left(\sum_{k=0}^{m}\binom{m}{k}y^{(k)}\left(\sum_{l=0}^{m-k}\binom{m-k}{l}z^{(l)}z^{(m-k-l)}\right)\right)g_7^{(n-m)} \tag{10}
$$

$$
z_{J_2}^{(n+2)} = 3\sum_{m=0}^{n}\binom{n}{m}z^{(m)}g_5^{(n-m)} - 5\sum_{m=0}^{n}\binom{n}{m}\left(\sum_{k=0}^{m}\binom{m}{k}z^{(k)}\left(\sum_{l=0}^{m-k}\binom{m-k}{l}z^{(l)}z^{(m-k-l)}\right)\right)g_7^{(n-m)} \tag{11}
$$

Hence, for the perturbed two-body problem higher order derivatives of $\mathbf{r}$ are evaluated as,

$$
\mathbf{r}^{(2+n)} = -\mu\sum_{m=0}^{n}\binom{n}{m}\boldsymbol{r}^{(m)}g_3^{(n-m)} + \mathrm{M}\begin{Bmatrix} x_{J_2}^{(2+n)} \\ y_{J_2}^{(2+n)} \\ z_{J_2}^{(2+n)} \end{Bmatrix} \tag{12}
$$

The analytic continuation solution is then applied utilizing (12) to evaluate higher order derivatives of $\mathbf{r}$ to obtain both the position and velocity components of the trajectory as,

$$
\begin{aligned}
\mathbf{r}\left(t+h\right) &= \mathbf{r}\left(t\right) + \dot{\mathbf{r}}h + \frac{\ddot{\mathbf{r}}h}{2!} + \frac{\dddot{\mathbf{r}}h^3}{3!} + \frac{\mathbf{r}^{(4)}h^4}{4!} + \cdots \\
\mathbf{v}\left(t+h\right) &= \dot{\mathbf{r}}\left(t\right) + \ddot{\mathbf{r}}h + \frac{\dddot{\mathbf{r}}h^2}{2!} + \frac{\mathbf{r}^{(4)}h^3}{3!} + \cdots
\end{aligned} \tag{13}
$$

As with any power series-based approximation one must come to grips with the issues: (1) how many terms need to be retained in the approximations, (2) how large can the step-size *h* be made for maintaining what level of position and velocity accuracy, (3) can variable step-size algorithms be developed for accelerating the series approximations, and (4) what is the computational performance of the series approximation when compared to other available approximation methods. The recursive nature of Eqs. (4), (6), (7),(9),(10), (11) are well suited for parallel implementations.

A Numerical Example

A case of a GEO circular orbit of 42241.12 km height is considered. The analytic continuation method is used and compared against *MATLAB® ODE45* and *RKN1210* in terms of accuracy and timing. Figure 1 and Figure 2 show the resulting comparison in accuracy between the analytic continuation method and *MATLAB®* standard *ODE45*.

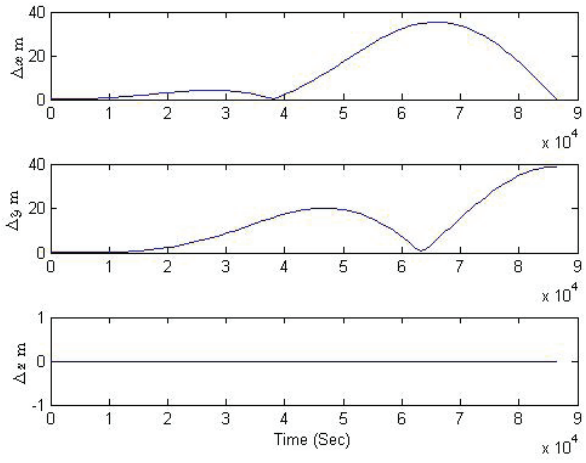

Figure 1: Position errors vs. *ode45*

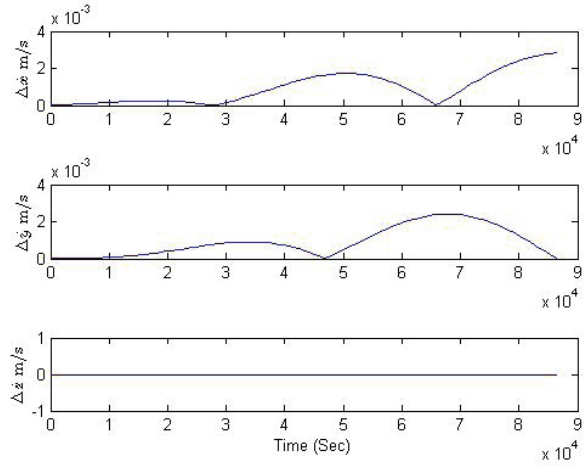

Figure 2: Velocity errors vs. *ODE45*

Figure 3 and Figure 4 show the resulting errors when compared with *RKN1210*. The error comparison shows that the analytic continuation method can achieve high accuracies as the number of steps is increased and consequently the step size is reduced. A timing comparison is conducted for the three integrators and the speed up achieved by the analytic continuation method is on average two orders of magnitude higher than both methods as shown in Figure 5.

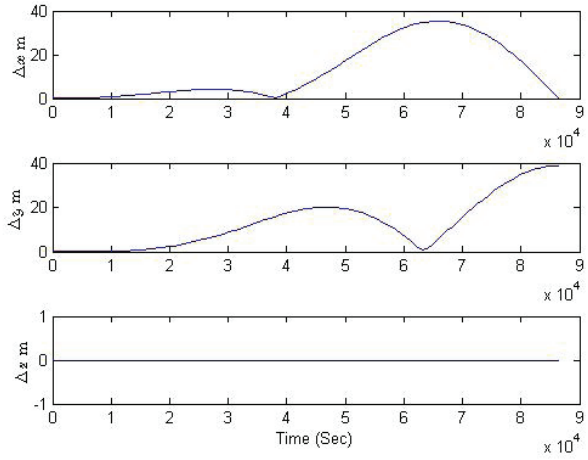

Figure 3: Position errors vs. *RKN1210*

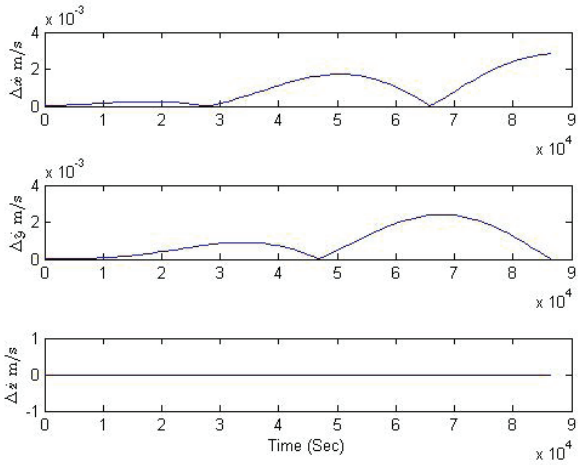

Figure 4: Velocity errors vs. *RKN1210*

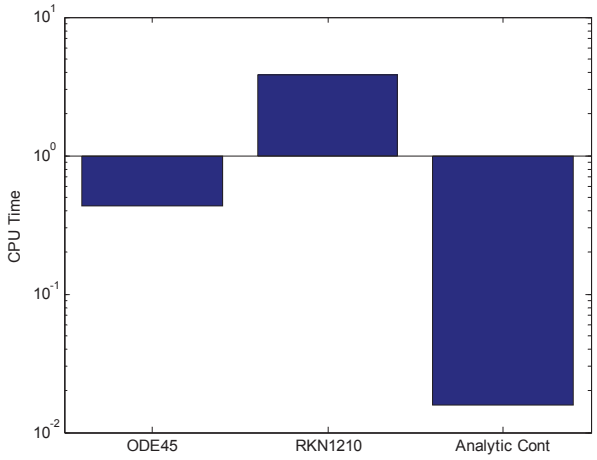

Figure 5: CPU Time Comparison

The speed up gained from employing the analytic continuation approach is quite significant whereas accuracy can be easily adjusted by increasing the number of time steps for the power series.

Though many more cases can be considered, the results presented above are typical. Additional cases are investigated in the following stability analysis section.

PADÉ APPROXIMATION AND SERIES CONVERGENCE

Padé series are used to better understand the series converging/diverging behavior for the analytic continuation method. Padé series algorithm replaces the analytical continuation Taylor series at each time step, [10] with a ratio of polynomials. For a series of N coefficients

$$f(x) = \sum_{k=0}^{N} C_k x^k, \tag{14}$$

a Padé series is obtained as

$$R(x) = \frac{\sum_{k=0}^{M} a_k x^k}{1 + \sum_{k=1}^{N} b_n x^k}, \tag{15}$$

for the case where $M = N$ coefficients of the Padé series are calculated by

$$\begin{aligned} \sum_{m=1}^{N} b_m C_{N-m+k} &= -C_{N+k}, \qquad k = 1, \cdots, N \\ \sum_{m=0}^{K} b_m C_{k-m} &= a_k, \qquad k = 1, \cdots, N \end{aligned} \tag{16}$$

The coefficients are calculated by solving the algebraic equations in (16) for the numerator a_k and the denominator b_k of the Padé series. The next step is to solve for the roots of the polynomial in the denominator to determine the series poles. This is done using numerical root finding methods that depend on the order of the polynomial and the order of the original Taylor series. For the x-axis part of the power series solution of the two-body problem the series coefficients are obtained at each time step as

$$x(t+\Delta t) = \underbrace{x(t)}_{C_0} + \underbrace{\dot{x}(t)}_{C_1}\Delta t + \underbrace{\frac{\ddot{x}(t)}{2!}}_{C_2}\Delta t^2 + \underbrace{\frac{\dddot{x}(t)}{3!}}_{c_3}\Delta t^3 + \cdots \tag{17}$$

With solutions available for the C_k coefficients, the Padé series coefficients are as defined in (16).

The convergence behavior of the trajectory model is examined by conducting an extensive numerical study involving a comparison between divergent and convergent power series solutions for the two-body problem.

NUMERICAL CASE STUDIES

Numerical experiments are conducted on two cases for solving the unperturbed two-body problem. The first case is a case of circular orbit which represents a converging series case that achieves mm accuracy with the minimum number of steps. The second case is a high eccentricity orbit, $e = 0.9$, that represents an inherently divergent case that requires a large number of steps and a relatively small step size to achieve high orbital prediction accuracy.

The convergent case

The same GEO circular orbit presented in the previous section is considered here. The initial position and velocity vectors are given by, $\mathbf{r} = \begin{bmatrix} 0 & 42241120 & 0 \end{bmatrix}^T$ m and $\dot{\mathbf{r}} = \begin{bmatrix} 0 & 3071.861 & 0 \end{bmatrix}^T$ m/s. Because the orbit is circular a closed form *F&G* solution exists. The analytic continuation solution is compared against the *F&G* solution for comparison of accuracy. The best achieved accuracy, i.e. the mm level, is found when dividing the orbit into 15 steps and taking 14 terms in the series, see Figure 6.

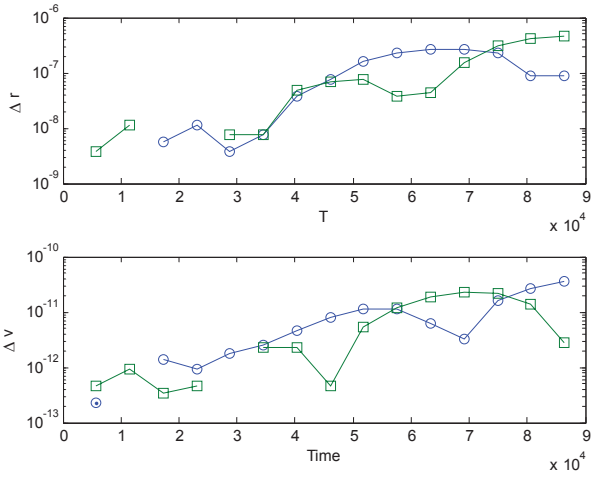

Figure 6: States Error, Convergent Case, Nstep = 15, Deriv = 14

Starting with the best result in terms of accuracy the number of series terms is varied and both the Padé series poles and the comparison with the closed form *F&G* solution is presented to give an insight about how convergence and pole behavior can be related. The following set of figures shows these results for 4, 6, 12 and 14 terms in the Taylor series.

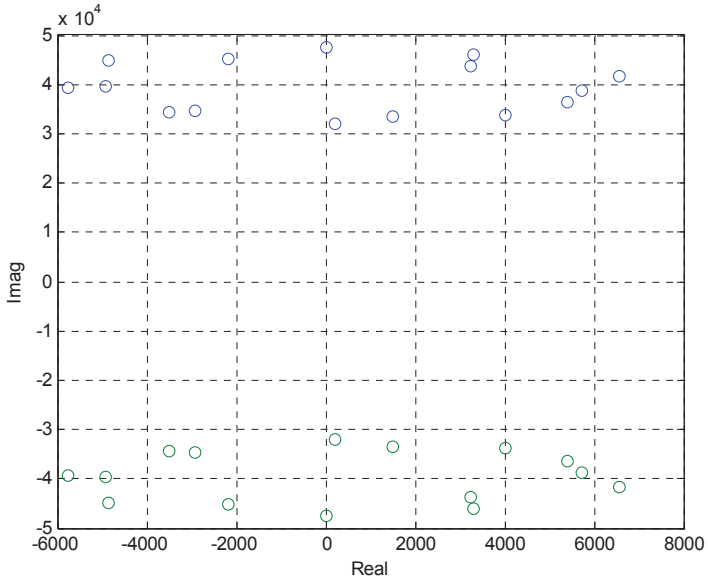

Figure 7: Pade Poles, Convergent Case, Nstep = 15, Deriv = 4

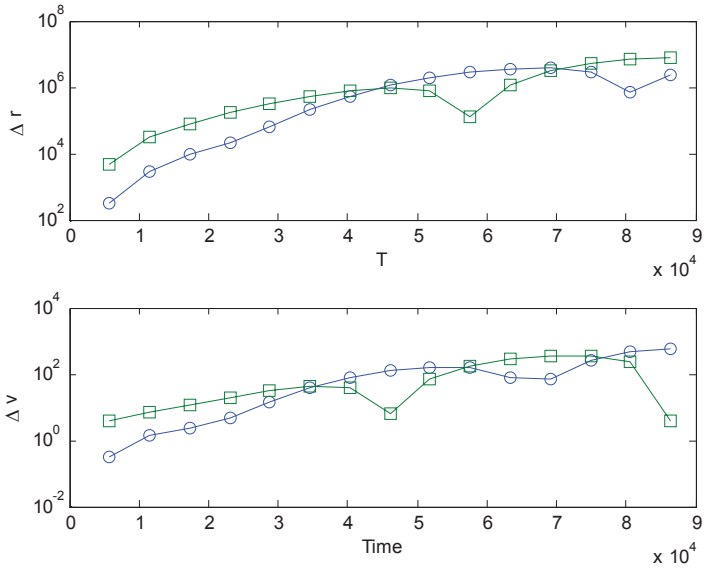

Figure 8: States Error, Convergent Case, Nstep = 15, Deriv = 4

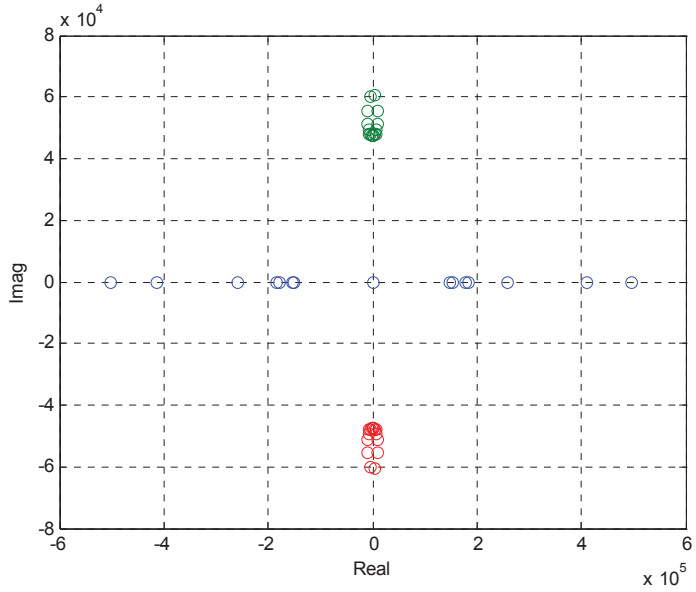

Figure 9: Pade Poles, Convergent Case, Nstep = 15, Deriv = 6

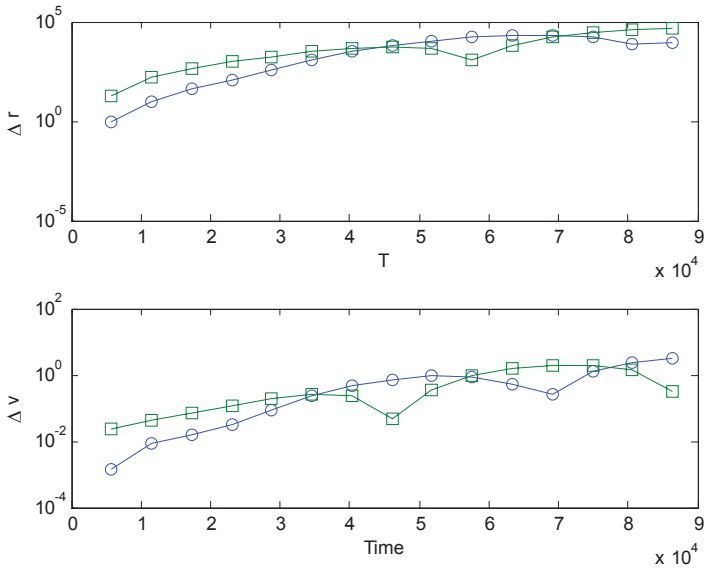

Figure 10: States Error, Convergent Case, Nstep = 15, Deriv = 6

Figure 8 and Figure 10 show an increase in accuracy by three orders of magnitude as the number of terms in the Taylor series is increased from 4 to 6. The associated change in the pattern of the Padé series poles is shown in Figure 7 and Figure 9. At 12 terms in the series a significant change in the pole patterns takes place, see Figure 11. As a consequence one observes 7 orders of magnitude improvement in the results as shown in Figure 12. Finally, at 14 terms in the series a significant improvement in the accuracy takes place that achieves mm accuracy, see Figure 14. The poles pattern also shows a significant change in the distribution as shown in Figure 13. As the number of terms in the series is increased no significant improvement in accuracy is observed. Also the poles distribution remains within the converging patterns shown and with no impact on accuracies. This may indicate saturation in the numerical precision allowed by the machine requiring a higher numerical precision experiment that can exploit the problem numerical precision to its full extent. It is also interesting to speculate on the transformation in the pole pattern observed at 12 terms, which corresponds to the limit of Runge-Kutta algorithms developed for celestial mechanics problems. Future research will attempt to dig deeper into the interpretation of the pole patterns observed.

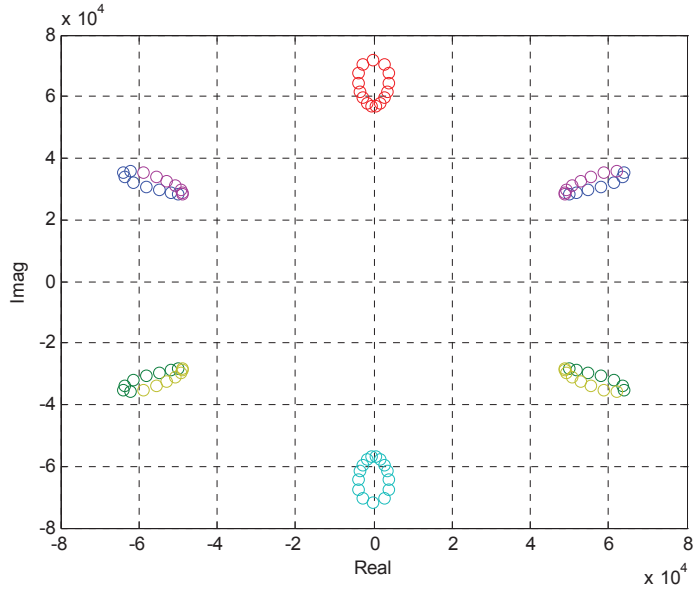

Figure 11: Pade Poles, Convergent Case, Nstep = 15, Deriv = 12

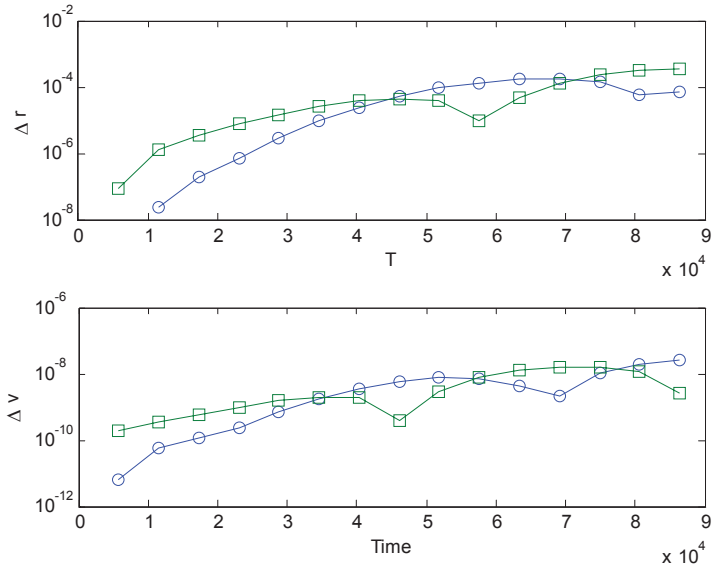

Figure 12: States Error, Convergent Case, Nstep = 15, Deriv = 12

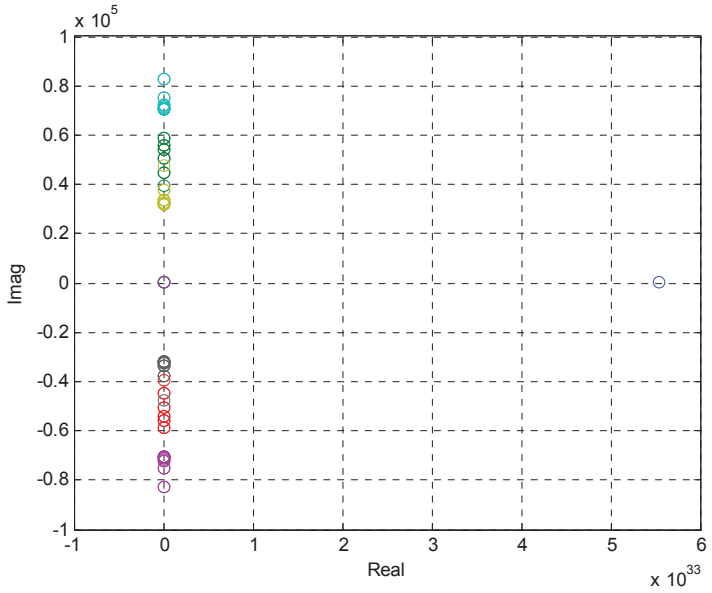

Figure 13: : Pade Poles, Convergent Case, Nstep = 15, Deriv = 14

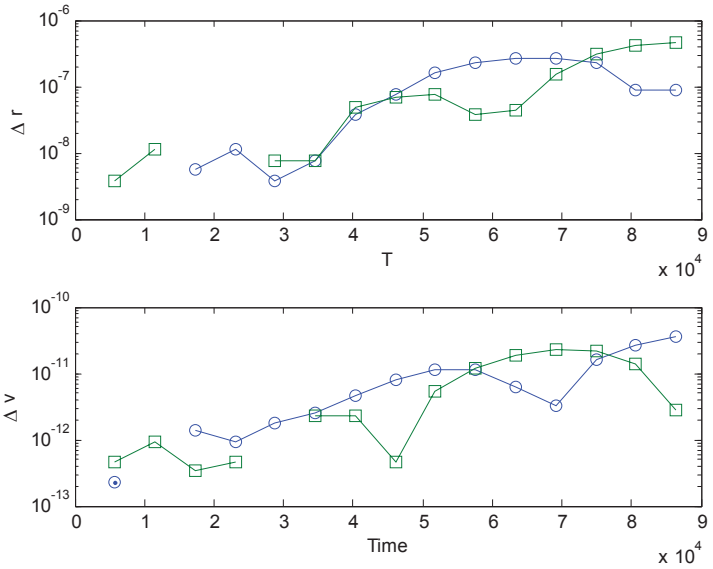

Figure 14: States Error, Convergent Case, Nstep = 15, Deriv = 14

The Divergent

This is a case of a very high eccentricity elliptical orbit, $e = 0.9$. The initial position and velocity vectors are given by, $\mathbf{r} = \begin{bmatrix} 7000000 & 0 & 0 \end{bmatrix}^T$ m and $\dot{\mathbf{r}} = \begin{bmatrix} 0 & 10401.526536 & 0 \end{bmatrix}^T$ m/s. This case is very sensitive and achieving high accuracies in position and velocity of the orbit is

extremely difficult. The analytic continuation approach is used as previously indicated. The number of terms in the series is fixed at 14 and the number of steps is increased until acceptable accuracy is achieved. The poles of the Padé approximation are plotted as the previous case and the errors between the initial and final states are added in a corresponding table. The first numerical experiment is done with 100 steps, Figure 15. The errors in that case are order of infinity, Table 1.

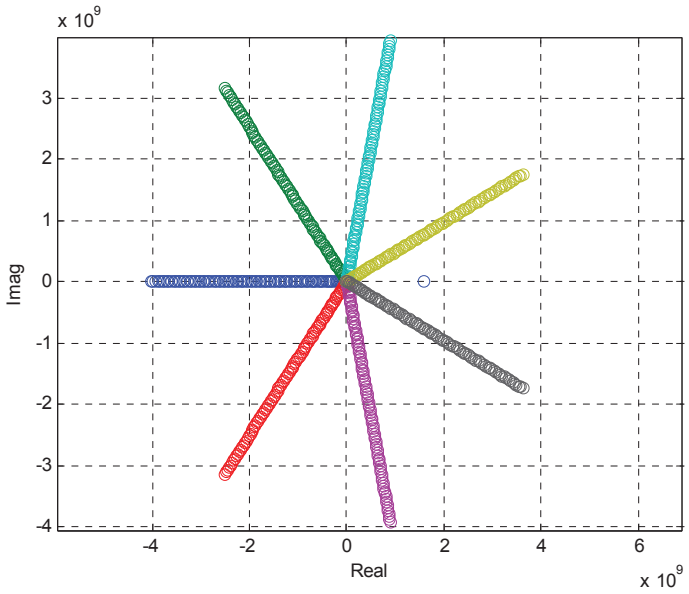

Figure 15: : Pade Poles, Divergent Case, Nstep = 100, Deriv = 14

Table 1: Error Single Orbit (m,m/s), Divergent Case, Nstep = 100, Deriv = 14

State	x	y	z	$\dot{x}$	$\dot{y}$	$\dot{z}$
Error	0.12E+19	0.1E+19	0.0	0.7E+13	0.6E+13	0.0

The Number of steps is then increased to 500. Still the same star like pattern exists for the Padé series poles, see Figure 16 but with a significant improvement on the final states errors, Table 2.

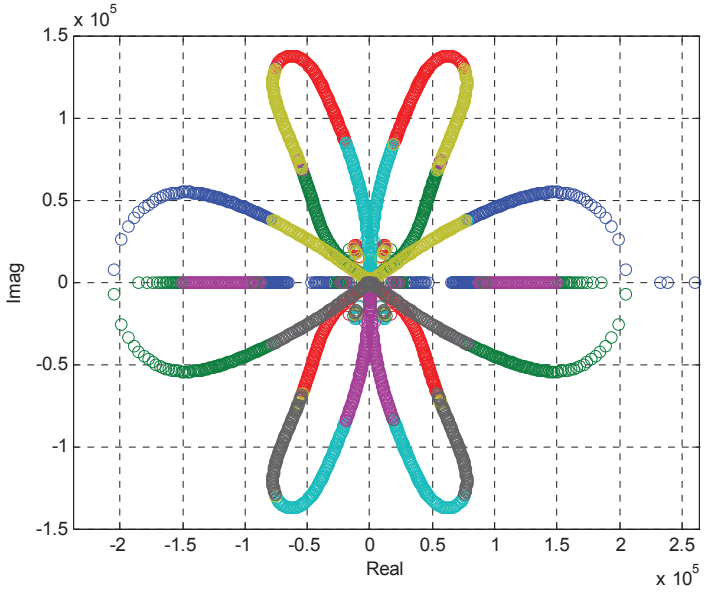

Figure 16: : Pade Poles, Divergent Case, Nstep = 500, Deriv = 14

Table 2: : Error Single Orbit (m,m/s), Divergent Case, Nstep = 500, Deriv = 14

State	x	y	z	$\dot{x}$	$\dot{y}$	$\dot{z}$
Error	0.151E+03	0.677E+05	0.0	0.509E+02	0.23010	0.0

The number of steps is further increased to 800. The poles of the Padé series are plotted as shown in Figure 17 and Figure 18 which shows the full picture of the pole placement with one pole existing way on the right at several orders of magnitude higher value than the rest of the poles for all time steps. Table 3 shows the error in the final states.

Table 3: Error Single Orbit (m,m/s), Divergent Case, Nstep = 800, Deriv = 14

State	x	y	z	$\dot{x}$	$\dot{y}$	$\dot{z}$
Error	0.365E-03	0.482E+02	0.0	0.377E-01	0.702E-06	0.0

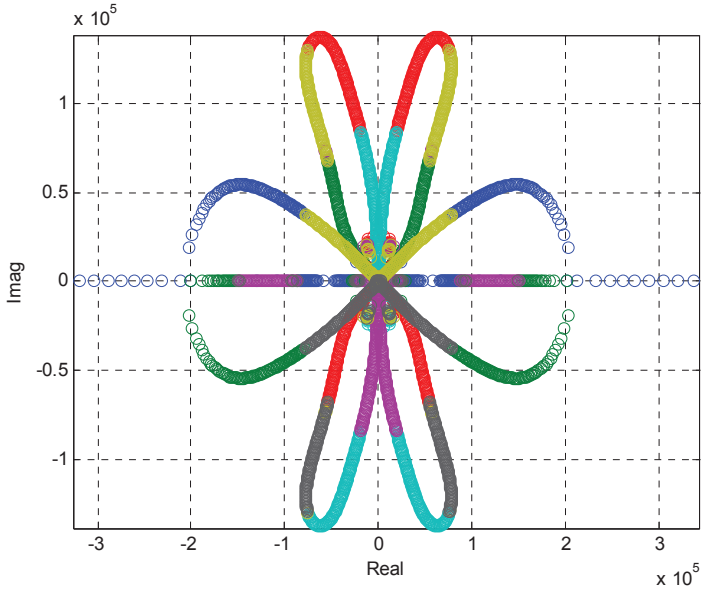

Figure 17: Pade Poles, Divergent Case, Nstep = 800, Deriv = 14 (Zoomed In)

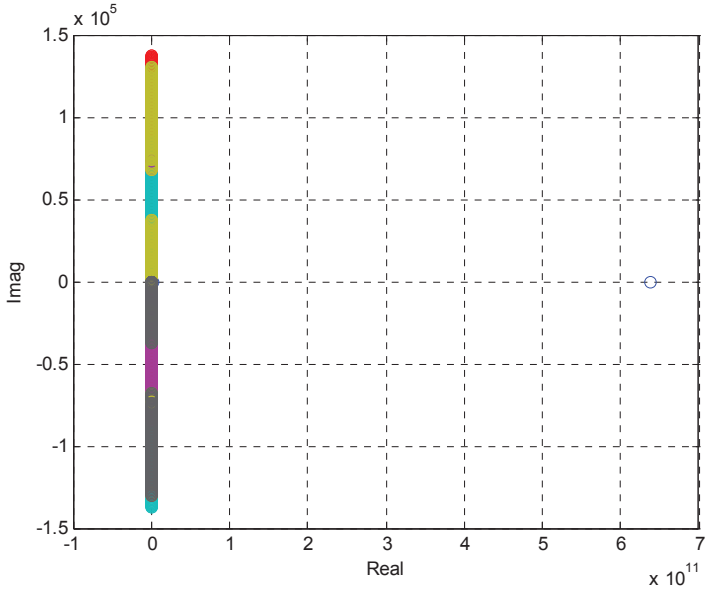

Figure 18: Pade Poles, Divergent Case, Nstep = 800, Deriv = 14

At this level accuracy is improving significantly with higher errors appearing in the y position state (3 orders of magnitude higher than the highest error). The number of steps are next increased further to improve the error in that state and investigate the effect of poles of Padé approximation in obtaining better results.

The next set of results are shown for 1250 steps.

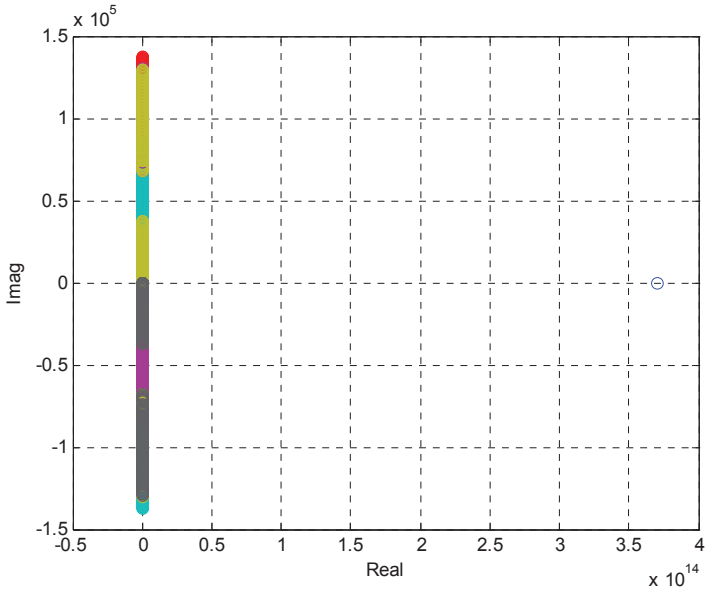

Figure 19: : Poles, Divergent Case, Nstep = 1250, Deriv = 14

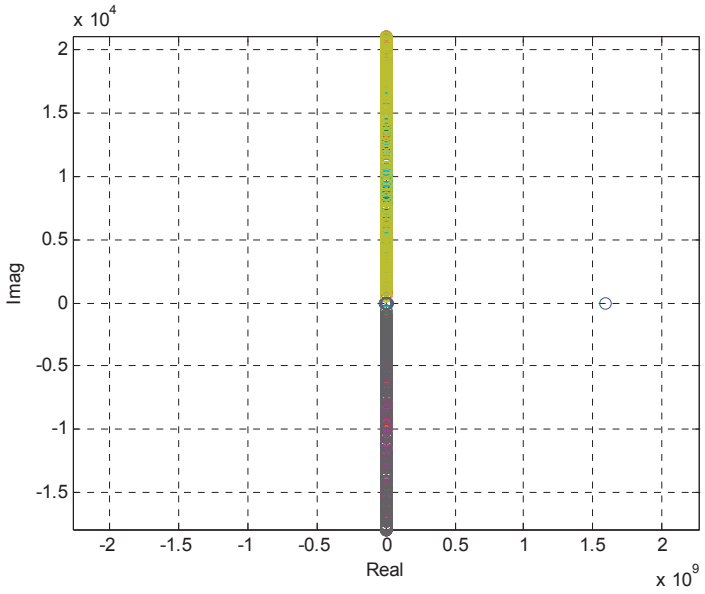

Figure 20: : Poles, Divergent Case, Nstep = 1250, Deriv = 14 (Zoomed In)

Table 4: Error Single Orbit (m,m/s), Divergent Case, Nstep = 1250, Deriv = 14

State	x	y	z	$\dot{x}$	$\dot{y}$	$\dot{z}$
Error	0.316E-07	0.833E-01	0.0	0.65E-04	0.200E-10	0.0

It is quite obvious that the star like pattern seized to exist, Figure 19 and Figure 20, and significant improvement in the errors is achieved,

Table 4 . The change in the poles behavior with improved accuracies for both the diverging and the converging case is quite formidable. The association of convergence to a certain existence of Padé poles pattern can be investigated further to better understand the correlation between both series approximations.

Accuracies and timing for this case are also investigated with *ODE45* and *RKN1210* versus the analytic continuation approach. Table 5 shows accuracy comparison results between the initial states and the final states for one complete orbital period. In this comparison the numerical methods are used with both standard tolerances for errors (10^{-6}) and the maximum tolerances allowed by the machine (10^{-13}) Timing plot comparison is shown in Figure 21.

Table 5: Initial vs. final states errors comparison

	Δx m	Δy m	Δz m	$\Delta \dot{x}$ m/s	$\Delta \dot{y}$ m/s	$\Delta \dot{z}$ m/s
ODE45 **(Std. tolerances)**	3201417.3	9156113.27	0	5044.6446	3380.322	0
ODE45 **(Max tolerances)**	1.061E-07	0.000335	0	2.62E-07	5.09E-11	0
RKN1210 **(Std. tolerances)**	4.060E-07	0.00016	0	1.325E-07	3.11E-10	0
RKN1210 **(Max tolerances)**	2.291E-07	0.000125	0	9.763E-08	1.655E-10	0
Analytic Continuation NStp = 1200	0.190E-06	0.00058	0	-0.454E-06	-0.13E-09	0

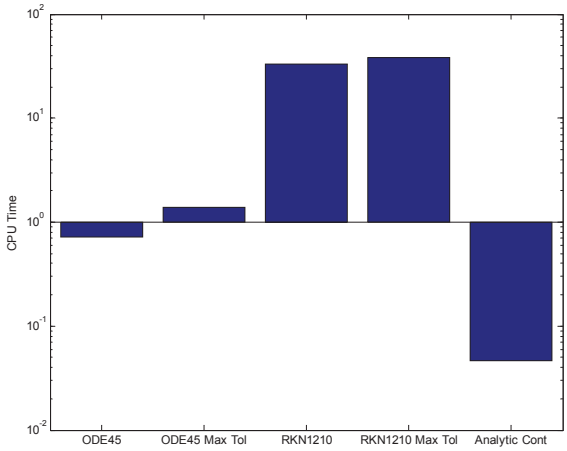

Figure 21: Timing study divergent case

The results show that for about three orders of magnitude speed up the analytic continuation achieves comparable accuracies to the most accurate numerical method available.

DISCUSSION AND CONCLUSION

The analytic continuation solution is extended to solve a broader case of problems to encompass the perturbed two-body problem for the Earth oblateness effects. This solution scheme can be easily extended to evaluate the higher perturbation harmonics as function of the predefined Lagrange-Like invariants. The speed and accuracy enabled by the power series solution is orders of magnitude better than the current standard numerical integrators in terms of speed while retaining the same accuracies.

Padé approximations provided new insights on the stability and the accuracy of the power series. The distinct change in the poles placements of the Padé series is an indication for the transition between convergence and divergence. Such patterns are investigated and qualitatively examined for their associations with specific series behaviors, though more research is required to fully understand the system-level numerical stability issues. The work presented in this area is a first step to better understand the convergence criteria for the two-body problem series expansion and can lead the way for a better understanding of Taylor series solution in general.

REFERENCES

[1] Battin, R. H. *An introduction to the mathematics and methods of astrodynamics*, AIAA, 1999.

[2] Lagrange, J. L. *Mécanique Analytique*. Paris: Gauthier-Villars, 1811.

[3] Brouwer, D., and Clemence, G. *M. Methods of celestial mechanics, New York Academic Press, 1961 Vol. 1, 1961.*

[4] Hamilton, W. R. "On a general method in dynamics," *Philosophical Transactions of the Royal Society* Vol. 2, 1834, pp. 247-308.

[5] Schaub, H., and Junkins, J. L. *Analytical mechanics of space systems*, AIAA, 2003.

[6] Turner, J.D., Elgohary, T.A., Majji, M. and Junkins, J.L. "Hight Accuracy Trajectory Uncertainty Propagation Algorithm for Long Term Asteroid Motion Prediction," Adventures on the Interface of Mechanics and Control. Tech Science Press, 2012.

[7] Pade approximation and its applications, proceedings of a conference held in Antwerp, Belgium, 1979.
[8] Amilcare, P. and Pozzi, A. *Applications of Padé approximation theory in fluid dynamics.* World Scientific, 1993.
[9] Michael Francis, P., and Pas, M. F. "Applications of the Pade approximant method in physical chemistry." Thesis (M.S.)--Texas A&M University, 1984.
[10] Press, W. H., Teukolsky, S. A., Vetterling, W. T., and Flannery, B. P. *Numerical recipes in FORTRAN*: Cambridge university press, 1994.